Toward an Understanding of the Mechanisms of the Intramolecular [5 + 2] Cycloaddition Reaction of γ-Pyrones Bearing Tethered Alkenes. A Theoretical Study

Luis R. Domingo* and Ramón J. Zaragozá

Departamento de Química Orgánica, Universidad de Valencia, Dr Moliner 50, 46100-Burjassot, Valencia, Spain

domingo@utopia.uv.es

Received January 14, 2000

The molecular mechanism for the intramolecular [5 + 2] cycloaddition reaction of β-silyloxy-γ-pyrones bearing tethered alkenes has been characterized using ab initio methods. A comparative study for this sort of cycloaddition carried out at different computational levels points out that the B3LYP/6-31G* calculations give similar barriers to those obtained with the MP3/6-31G* level. Analysis of the energetic results shows that the reaction takes place along a stepwise process: first, the migration of the neighboring silyl group to the carbonyl group of the γ-pyrone takes place to give a weak oxidopyrylium ylide intermediate, which by a subsequent concerted intramolecular [5 + 2] cycloaddition affords the final cycloadduct. The cycloaddition process is very stereoselective due to the constraints imposed by the tether. The [5 + 2] cycloaddition reaction has a large barrier, and the presence of the silyloxy group and the intramolecular character of the process are necessary to ensure the thermodynamic and kinetic feasibility of these cycloadditions.

Introduction

A major challenge in contemporary organic synthesis is to devise methods and strategies for the rapid and economic preparation of highly complex molecules from simple starting materials. Among the alternative approaches to meet this challenge, those based on methods that allow the simultaneous creation of several bonds in a single operation, such as cycloaddition reactions, are particularly appealing.[1]

Thus, the thermolysis of substituted β-hydroxy-γ-pyrones bearing tethered alkenes, which allows the internal [5 + 2] cycloaddition to give relatively complex 8-oxabicyclo[3.2.1]octane systems, can be considered as an example of this challenge (see Scheme 1).[2,3] The rich functionalization and stereochemical bias of these frameworks favor a rapid conversion into a variety of valuable structures. Thus, the oxidative cleavage of the carbocycle system allows the synthesis of *cis*-2,5-disubstituted tetrahydrofurans.[3]

Wender and Mascareñas proposed that the formation of the oxidopyrylium ylide **I**, which is generated in situ through the migration of the group present on the O-3 oxygen atom to the O-4 oxygen atom, is the key of this [5 + 2] cycloaddition (see Scheme 1).[4] The *tert*-butyldimethylsilyl ether (TBSO) has been used as a good migratory group (see Scheme 2).[3] Under thermolysis conditions this group can migrate from the O-3 to the O-4 position, generating the corresponding oxidopyrylium ylide and promoting the subsequent intramolecular [5 + 2] cycloaddition. However, the cycloaddition process involving a pentacoordinate silicate has not been discarded.[5]

The consecutive nature of this chemical process does not allow establishment of the molecular mechanism of the reaction, and the question if the migration of the silyl ether is simultaneous to the cycloaddition reaction remains unresolved. Consequently, the study of the mechanism is necessary in order to know as this sort of cycloaddition reactions takes place.

The structural information obtained by theoretical methods based on quantum mechanical calculations of possible intermediates and transition structures (TSs) provide powerful assistance for the study of organic reaction mechanisms.[6] These methods are accepted as available tools for the interpretation of experimental results, since such data are rarely available from experiments.[6d]

Our research program has long maintained an interest in the study of the mechanism of cycloaddition reactions, and the understanding of the characteristic feature of these [5 + 2] cycloadditions prompted us to explore the mechanistic aspects.

In the present study the intramolecular [5 + 2] cycloaddition reaction of the β-silyloxy-γ-pyrone **1** bearing a tethered alkene to give the cycloadduct **2**, as a model of the reaction reported by Mascareñas et al.,[3] has been studied using ab initio methods in order to characterize the mechanism of this sort of cycloaddition process and to understand the stereochemical outcomes (see Scheme 3).

Computational Methods

All calculations were carried out with the Gaussian 98 suite of programs.[7] An exhaustive exploration of the potential energy

(1) Carruthers, W. *Cycloaddition Reactions in Organic Synthesis*; Pergamon: Oxford, 1990.

(2) Rumbo, A.; Castedo, L.; Mouriño, A.; Mascamareñas, J. L. *J. Org. Chem.* **1993**, *58*, 5585.

(3) Rodríguez, J. R.; Rumbo, A.; Castedo, L.; Mascamareñas, J. L. *J. Org. Chem.* **1999**, *64*, 4560.

(4) Wender, P. A.; Mascareñas, J. L. *Tetrahedron Lett.* **1992**, *33*, 2115.

(5) Wender, P. A.; McDonald, F. E. *J. Am. Chem. Soc.* **1990**, *112*, 4956.

(6) (a) Tapia, O.; Andrés, J. *Chem. Phys. Lett.* **1984**, *109*, 471. (b) Willians, I. H. *Chem. Soc. Rew.* **1993**, 227. (c) Houk, K. N.; González, J.; Li, Y. *Acc. Chem. Res.* **1995**, *28*, 81. (d) Wiest, O.; Montiel, D. C.; Houk, K. N. *J. Phys. Chem. A* **1999**, 8378.

10.1021/jo000061f CCC: $19.00
Published on Web 08/15/2000

Scheme 1

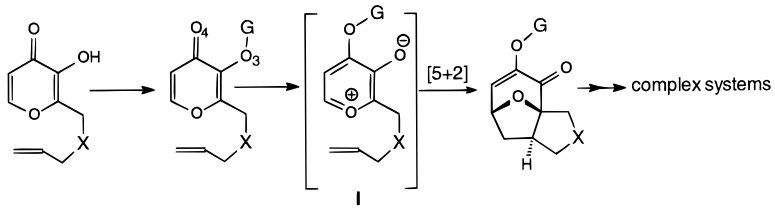

Scheme 2

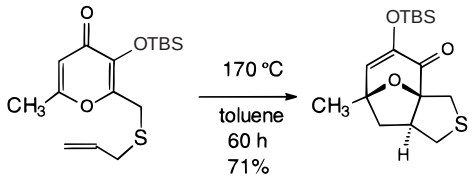

surface (PES) was carried out at the HF/3-21G level[8] to ensure that all relevant stationary points were located and properly characterized. The optimizations were carried out using the Berny analytical gradient optimization method.[9] The stationary points were characterized by frequency calculations in order to verify that minima and transition structures have zero and one imaginary frequency, respectively. The HF/3-21G frequencies were used as starting point in the search of the HF/6-31G* structures.

Previous theoretical studies of [4 + 2] and related cycloaddition reactions have indicated that the activation energies calculated at the HF level are too large, whereas MP2 calculations tend to underestimate them. However, energy calculations for stationary points using MP3/6-31G* are in accord with experimental values.[10] Recently, DFT calculations using the B3LYP hybrid functional[11] have been shown to be in good agreement with experimental activation energy values[12] and to give a similar potential energy barrier (PEB) to that obtained using time-consuming MP3 calculations.[12d,e,j] Consequently, all HF/6-31G* stationary points were optimized at B3LYP/6-31G* level, to obtain accurate energies for a correct characterization of the PES.

The transition vectors (TV),[13] i.e., the eigenvector associated to the unique negative eigenvalue of the force constants matrix, have been characterized. The electronic structures of stationary points were analyzed by the natural bond orbital (NBO) method.[14]

The computed values of activation enthalpies, entropies and Gibbs energies have been estimated by means of the B3LYP/6-31G* PEBs along with the harmonic frequencies. These frequencies have been scaled by 0.96.[15] The activation Gibbs energies have been computed at 170 °C.[3] The enthalpy and entropy changes are calculated from standard statistical thermodynamic formulas.[8,10a]

Results and Discussions

(i) Energies. For the intramolecular cycloaddition reaction of the β-silyloxy-γ-pyrone **1**, three reaction modes are possible (see Scheme 3): in mode I the process is initialized by the transfer of the trimethylsilyl group from the initial O7 position to O9 one with formation of an oxidopyrylium ylide intermediate **IN1**. The subsequent intramolecular [5 + 2] cycloadditions of this intermediate afford the final cycloadducts **2** and **3**. In mode II the process in initialized by intramolecular [5 + 2] cycloadditions of **1** to afford the intermediates **IN2** or **IN3**. The transfer of the trimethylsilyl group on these intermediates affords the final cycloadducts **2** and **3**. In mode III a simultaneous transfer of the trimethylsilyl group and cycloaddition process afford the final cycloadducts without participation of any intermediate. Finally, the cycloaddition processes can take place along both faces of the γ-pyrone system of **1**, yielding a pair of enantiomeric cycloadducts.

In Scheme 3 the stationary points corresponding to the three reaction modes have been presented together with the atom numbering, while the geometries of the TSs corresponding to these chemical conversions along the different reaction pathways are depicted in Figure 1. The relative energies are summarized in Table 1. In Figure 2 a schematic representation of the different energy profiles for the cycloaddition reaction is depicted.

As was stated in computational methods, the PEBs computed for [4 + 2] and related cycloadditions are very dependent on the computational model, the MP3 and B3LYP levels being in good agreement with experimental barriers. However, the large molecular system of **1**, together with the presence of the silicon and sulfur atoms preclude the MP3/6-31G* calculations. To test the help-

(7) Frisch, M. J.; Trucks, G. W.; Schlegel, H. B.; Scuseria, G. E.; Robb, M. A.; Cheeseman, J. R.; Zakrzewski, V. G.; Montgomery, J., J. A.; Stratmann, R. E.; Burant, J. C.; Dapprich, S.; Millam, J. M.; Daniels, A. D.; Kudin, K. N.; Strain, M. C.; Farkas, O.; Tomasi, J.; Barone, V.; Cossi, M.; Cammi, R.; Mennucci, B.; Pomelli, C.; Adamo, C.; Clifford, S.; Ochterski, J.; Petersson, G. A.; Ayala, P. Y.; Cui, Q.; Morokuma, K.; Malick, D. K.; Rabuck, A. D.; Raghavachari, K.; Foresman, J. B.; Cioslowski, J.; Ortiz, J. V.; Stefanov, B. B.; Liu, G.; Liashenko, A.; Piskorz, P.; Komaromi, I.; Gomperts, R.; Martin, R. L.; Fox, D. J.; Keith, T.; Al-Laham, M. A.; Peng, C. Y.; Nanayakkara, A.; Gonzalez, C.; Challacombe, M.; W. Gill, P. M.; Johnson, B.; Chen, W.; Wong, M. W.; Andres, J. L.; Gonzalez, C.; Head-Gordon, M.; Replogle, E. S.; Pople, J. A. Gaussian 98, Revision A.6, Gaussian, Inc., Pittsburgh, PA, 1998.

(8) Hehre, W. J.; Radom, L.; Schleyer, P. v. R.; Pople, J. A. *Ab initio Molecular Orbital Theory*; Wiley: New York, 1986.

(9) (a) Schlegel, H. B. *J. Comput. Chem.* **1982**, *3*, 214. (b) Schlegel, H. B. Geometry Optimization on Potential Energy Surface. In *Modern Electronic Structure Theory*; Yarkony D. R., Ed.; Singapore, 1994.

(10) (a) Jorgensen, W. L.; Lim, D.; Blake, J. F. *J. Am. Chem. Soc.* **1993**, *115*, 2936. (b) Sbai, A.; Branchadell, V.; Oliva, A. *J. Org. Chem.* **1996**, *61*, 621. (c) Domingo, L. R.; Picher, M. T.; Andrés, J.; Safont, V. S. *J. Org. Chem.* **1997**, *62*, 1775.

(11) (a) Becke, A. D. *J. Chem. Phys.* **1993**, *98*, 5648. (b) Lee, C.; Yang, W.; Parr, R. G. *Phys. Rev. B* **1988**, *37*, 785.

(12) (a) Stanton, R. V.; Merz, K. M. *J. Chem. Phys.* **1994**, *100*, 434. (b) Carpenter, J. E.; Sosa, C. P. *J. Mol. Struct. (THEOCHEM)* **1994**, *311*, 325. (c) Baker, J.; Muir, M.; Andzelm, J. *J. Chem. Phys.* **1995**, *102*, 2036. (d) Jursic, B.; Zdravkovski, Z. *J. Chem. Soc., Perkin Trans 2* **1995**, 1223. (e) Goldstein, E.; Beno, B.; Houk, K. N. *J. Am. Chem. Soc.* **1996**, *118*, 6036. (f) Branchadell, V. *Int. J. Quantum Chem.* **1997**, *61*, 381. (g) Sbai, A.; Branchadell, V.; Ortuño, R. M.; Oliva, A. *J. Org. Chem.* **1997**, *62*, 3049. (h) Branchadell, V.; Font, J.; Moglioni, A. G.; Ochoa de Echaguen, C.; Oliva, A.; Ortuno, R. M.; Veciana, J.; Vidal Gancedo, J. *J. Am. Chem. Soc.* **1997**, *119*, 9992. (i) García, J. I.; Martínez-Merino, V.; Mayoral, J. A.; Salvatella, L. *J. Am. Chem. Soc.* **1998**, *120*, 2415. (j) Domingo, L. R.; Arnó, M.; Andrés, J. *J. Am. Chem. Soc.* **1998**, *120*, 1617. (k) Domingo, L. R.; Picher, M. T.; Zaragozá, R. J. *J. Org. Chem.* **1998**, *63*, 9183. (l) Morao, I.; Lecea, B.; Cossió, F. P. *J. Org. Chem.* **1997**, *62*, 7033. (m) Domingo, L. R.; Arnó, M.; Andrés, J. *J. Org. Chem.* **1999**, *64*, 5867.

(13) (a) McIver, J. W. J.; Komornicki., A. *J. Am. Chem. Soc.* **1972**, *94*, 2625. (b) McIver, J. W. J. *Acc. Chem. Res.* **1974**, *7*, 72.

(14) (a) Glendening, E. D.; Reed, A. E.; Carpenter, J. E.; Weinhold, F.; NBO version 3.1 in Gaussian 98, Revision A.6. (b) Reed, A. E.; Weinstock, R. B.; Weinhold, F. *J. Chem. Phys.* **1985**, *83*, 735. (c) Reed, A. E.; Curtiss, L. A.; Weinhold, F. *Chem. Rev.* **1988**, *88*, 899.

(15) Scott, A. P.; Radom, L. *J. Phys. Chem.* **1996**, *100*, 16502.

Scheme 3

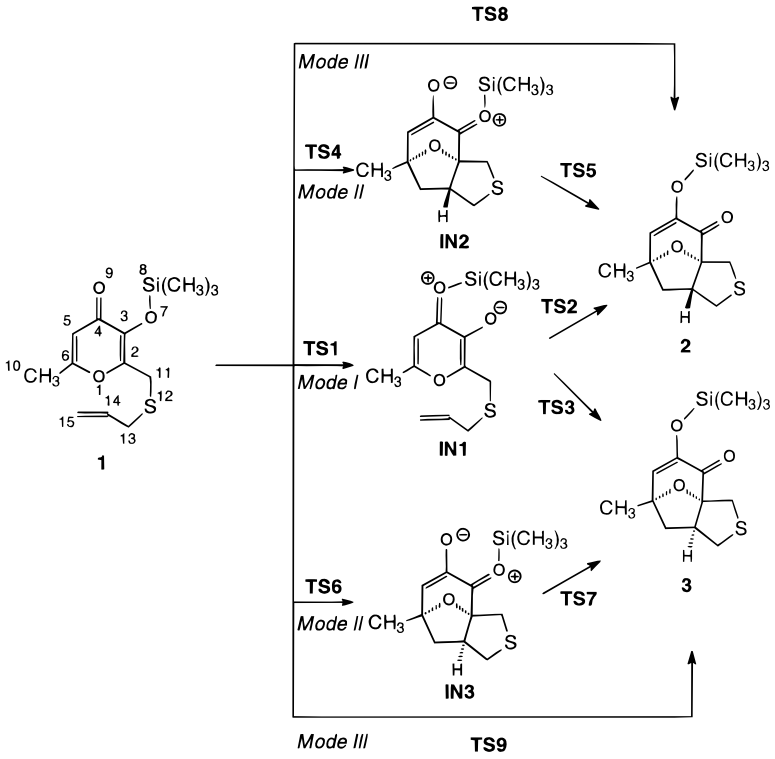

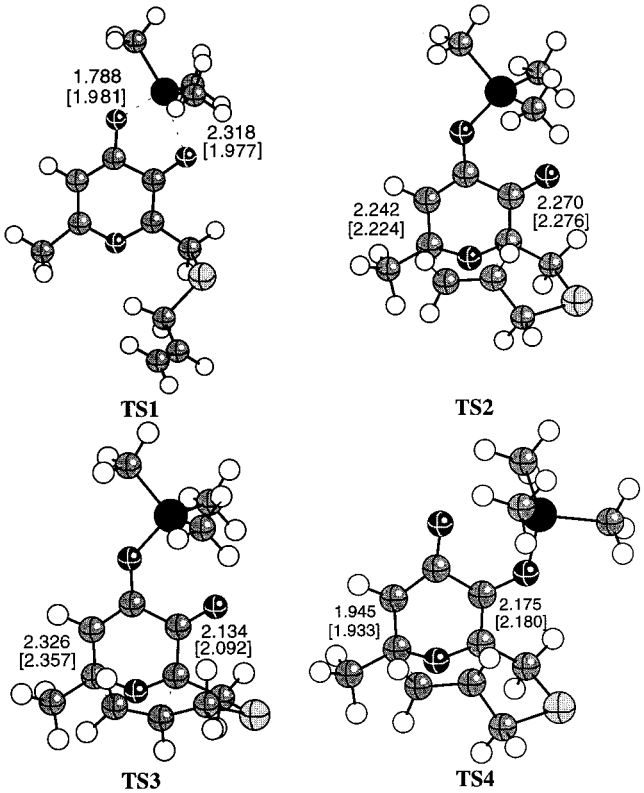

Figure 1. Selected geometrical parameters for the transition structures corresponding to the intramolecular [5 + 2] cycloaddition of the γ-pyrone **1**. The values of the lengths of the bonds directly involved in the reaction obtained at the RHF/6-31G* and B3LYP/6-31G* (in brackets) are given in angstroms.

Table 1. Relative Energies[a] (kcal/mol) for the Stationary Points of the Intramolecular [5 + 2] Cycloaddition Reaction of the γ-Pyrone 1

	HF/6-31G*	B3LYP/6-31G*
TS1	24.5	14.1
IN1	24.2	12.2
TS2	53.6	29.6
TS3	65.7	39.3
TS4	64.6	39.5
2	−16.8	−10.6
3	−3.0	1.1

[a] Relative to **1**.

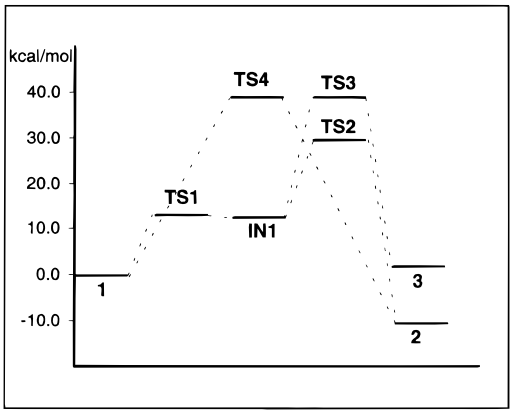

Figure 2. A schematic representation of the energy profiles for the intramolecular [5 + 2] cycloaddition reaction of the γ-pyrone **1**.

fulness of the B3LYP/6-31G* level, the PEB corresponding to the [5 + 2] cycloaddition of a reduced model, the oxidopyrylium ylide **IN4** and propene **5**, has been studied at different computational levels (see Scheme 4). Figure 3 shows the geometry of the **TS10** corresponding to the intermolecular [5 + 2] cycloaddition between the oxidopyrylium ylide **IN4** and **5**, while Table 2 presents the energetic results.

The values of the PEBs presented in Table 2 show an important dependency on the calculation level. While the

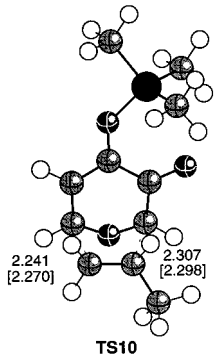

Figure 3. Selected geometrical parameters for the transition structure **TS10** corresponding to the intermolecular [5 + 2] cycloaddition between **IN4** and **5**. The values of the lengths of the bonds directly involved in the reaction obtained at the RHF/6-31G* and B3LYP/6-31G* (in brackets) are given in angstroms.

Scheme 4

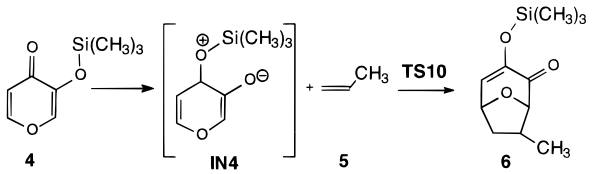

Table 2. Relative Energies[a] (kcal/mol) for the Transition Structure TS10 Corresponding to the Intermolecular [5 + 2] Cycloaddition Reaction of IN4 + 5

	TS10
HF/6-31G*	29.0
B3LYP/6-31G*	16.1
MP2/6-31G*//B3LYP/6-31G*	5.5
MP3/6-31G*//B3LYP/6-31G*	13.2

[a] Relative to **IN4** + **5.**

HF/6-31G* level presents the larger barrier, the inclusion of electron correlation energy at the MP2 level leads to a significant decrease of the energy barrier. The inclusion of electron correlation energy up to the MP3 level leads to reasonable value of the activation parameter. This fact shows that MP2 calculations overestimate the effect of the electron correlation energy on the transition structure with respect to that of the reactants. Finally, B3LYP/6-31G* calculations afford a similar result to that obtained with the very expensive MP3 level. This trend is similar to that found for [4 + 2] cycloadditions.[10a,c,12d,e,j,16] Thus, this preliminary study allows to assert the use the B3LYP/6-31G* method in order to obtain accurate barrier heights.

For the reaction along the mode I (see Scheme 3), the first step is the migration of the trimethylsilyl group from the O7 position to O9 one, with formation of the oxidopyrylium ylide intermediate **IN1**, via the **TS1**. The PEB associated with this process is 14.1 kcal/mol; the formation of the intermediate **IN1** is very endothermic, 12.2 kcal/mol (energetic data correspond to B3LYP/6-31G* results). In consequence, the intermediate **IN1** is very unstable, and with a very low barrier it is quickly converted in **1**.

Due to the free rotation of the chain of the C2 tethered alkene, the intermediate **IN1** can undergo also two intramolecular [5 + 2] cycloadditions to give the cycloadducts **2** and **3**, via the **TS2** and **TS3**, respectively. These cycloadditions are related with the *exo* and *endo* approaches of the terminal double bond to the C2 and C6 position of γ-pyrone **1**. The PEBs associated with these cycloaddition processes are 17.4 and 27.1 kcal/mol, respectively; the barrier for the transformations of γ-pyrone **1** into the cycloadducts **2** and **3** are 29.6 and 39.3 kcal/mol, respectively. These energies are very large and allow to explanation of the high temperature required for this sort of cycloaddition reaction. The larger PEB associated with **TS3** relative to **TS2** (9.7 kcal/mol) is due to the constraints imposed by the tether along the *endo* approach and justify the total *exo* stereoselectivity found in this cycloaddition process. The formation of the cycloadduct **2** is an exothermic process, −10.6 kcal/mol, whereas formation of the cycloadduct **3** is lightly endothermic, 1.1 kcal/mol. Thus, formation of **3** is kinetic and thermodynamically unfavored and justify the unique formation of **2**.

Table 3. Activation Enthalpies (in kcal/mol), Entropies (in cal/mol·K) and Gibbs Energies (in kcal/mol) Computed at 170 °C and 1 Atm for the Intramolecular [5 + 2] Cycloaddition of the γ-Pyrone 1, and the Intermolecular [5 + 2] Cycloaddition between 4 and 5

	$\Delta H^{\ddagger}$	$\Delta S^{\ddagger}$	$\Delta G^{\ddagger}$
IN1 → 2	16.3	−18.9	24.7
1 → 2	28.2	−17.7	36.0
IN4 + 5 → 6	17.0	−43.8	36.4
4 + 5 → 6	29.9	−44.7	49.7

For the reaction along the mode II (see Scheme 3), the process is initialized by the *exo* or *endo* intramolecular [5 + 2] cycloaddition of the γ-pyrone **1**, via **TS4** and **TS6**. The PEB associated with **TS4** is very large, 39.5 kcal/mol, it being similar to that for the formation of the nonobserved cycloadducts **3** via **TS3**. Consequently, this energetic result allows us to discount the direct [5 + 2] cycloaddition without the participation of the trimethylsilyloxy group. Moreover, all attempts to locate the intermediate **IN2** were unsuccessful. Although **TS4** is mainly associated to the C6−C15 and C2−C14 bond formation process (see later), this TS carried out directly the cycloadduct **2** without the participation of any intermediate. Finally, the large expected PEB for **TS6** relative **TS4**, due to the constraints imposed by the tether along the *endo* approach, allows us to discount the study of the reactive channel corresponding to formation of **3** along the mode II.

For the reaction along the mode III (see Scheme 3), the process corresponds to the [5 + 2] cycloaddition of the γ-pyrone **1** with simultaneous migration of the trimethylsilyl group, involving a pentacoordinated silicate.[5] However, all attempts to locate the transition structure **TS8** were unsuccessful. A careful exploration of the PES does not allow to locate the corresponding stationary point, giving structures more energetic than **TS2**, between 3 and12 kcal/mol. In consequence, the simultaneous migration of the trimethylsilyl group and [5 + 2] cycloaddition of **1** was discounted.

The values of activation enthalpies, entropies, and Gibbs energies, corresponding to the most favorable reactive channel with formation of **2**, have been estimated by means of the potential energy barriers computed at the B3LYP/6-31G* level along with the B3LYP/6-31G* harmonic frequencies. The activation Gibbs energies have been computed at 170 °C, which is the experimental temperature for this intramolecular [5 + 2] cycloaddition reaction.[3] The results are summarized in Table 3.

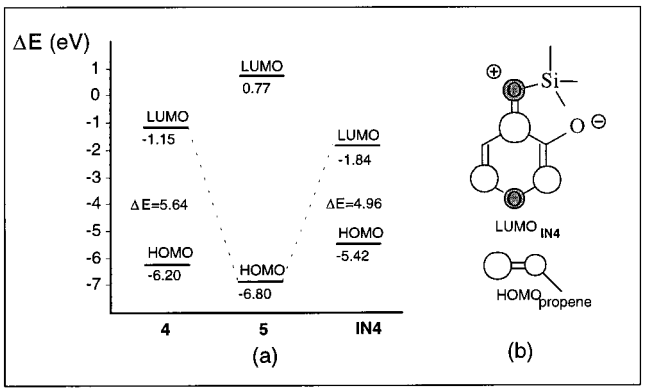

Figure 4. FMO interactions on the intermolecular [5 + 2] cycloadditions between propene **5** and the γ-pyrone **4**, or the oxidopyrylium ylide **IN4**.

The inclusion of the zero-point energy and thermal contributions leads to a small decrease of the potential energy barrier for the [5 + 2] cycloaddition process. However, the negative activation entropy corresponding to the intramolecular cycloaddition process, −18.9 cal/mol·K, is responsible for the rise of the activation Gibbs energy to 24.7 kcal/mol. The **1** → **2** process presents a very large activation Gibbs energy, 36.0 kcal/mol, and justifies the high temperature required experimentally to make feasible the cycloaddition process.[17]

The intermolecular [5 + 2] cycloaddition between **IN4** and **5** presents an activation enthalpy similar to that of the intramolecular one. However, the large negative activation entropy associated with the intermolecular process together with the high reaction temperature is responsible for the large activation Gibbs energy associated with this intermolecular cycloaddition mode, 36.4 kcal/mol; the **4** + **5** → **6** process has an activation Gibbs energy of 49.7 kcal/mol. This very large value reander the intermolecular [5 + 2] cycloaddition unfeasible and explains the demand of an intramolecular process using tethered alkenes.

The frontier molecular orbital (FMO) analysis allows us to understand the nature of these [5 + 2] cycloadditions (See Figure 4a). An analysis of the FMO for propene **5** and the γ-pyrone **4** indicates that the most favorable interaction along the cycloaddition process takes place between $HOMO_{propene}$ and $LUMO_{pyrone}$, the energy gap being very large ΔE = 5.64 eV. For the oxidopyrylium ylide **IN4** there is a decrease of the LUMO energy relative to that at the γ-pyrone **4**. This fact decreases of the $HOMO_{propene}$−$LUMO_{IN4}$ energy gap (ΔE = 4.96 eV), favoring the [5 + 2] cycloaddition. Finally, a representation of the more relevant $HOMO_{propene}$ and $LUMO_{IN4}$ molecular orbitals shows the favorable overlap that appears between the carbons atoms that participate in the two bond formation processes (see Figure 4b).

(ii) Geometrical Parameters and Analysis of Frequencies. A comparison of the geometrical parameters presented in Figure 1 indicates that for the cycloadditions the geometries obtained at the HF/6-31G* level are close to those obtained at the B3LYP/6-31G* one, showing similar bond formation processes.

For **TS1**, corresponding to the migration of the trimethylsilyl group from the O7 position to O9 one, the lengths of the O7−Si8 and O9−Si8 breaking and forming bonds are 1.977 and 1.981 Å, respectively, whereas in the intermediate **IN1** they are are: 2.833 and 1.749 Å (geometrical data correspond to B3LYP/6-31G* results). These data indicate that **TS1** corresponds to a synchronous process.

The lengths of the two σ-bonds being formed along the *exo* and *endo* [5 + 2] cycloaddition processes of the mode I are 2.224 Å (C6−C15) and 2.276 Å (C2−C14) at **TS2**, and 2.357 Å (C6−C15) and 2.092 Å (C2−C15) at **TS3**. These geometrical data indicate that both TSs correspond to concerted processes where the two σ-bonds are symmetrically formed. **TS3** is slightly more asymmetric than **TS2** due to the strain imposed by the tethered alkene along the *endo* approach. This strain, which is also present in the cycloadduct **3**, is responsible that **TS3** is 10 kcal/mol more energetic than **TS2**.

The lengths of the two σ-bonds being formed at **TS4** are: 1.933 Å (C6−C15) and 2.180 Å (C2−C14). These geometrical data indicate that this TS is slightly more asymmetric and more advanced that **TS2**. The O7−Si8 bond length, 1.767 Å, and Si8−O9 distance, 2.685 Å, are similar to those in **1**, indicating the nonparticipation of the trimethylsilyl group on the [5 + 2] cycloaddition process along the mode II.

In Table 4, the imaginary frequency, the main TV components and their corresponding geometric parameters for the TSs associated with the [5 + 2] cycloaddition processes are reported. The dominant TV components of these TSs, **TS2**, **TS3**, and **TS4**, are associated with the C2−C14 and C6−C15 σ-bonds which are being formed in these cycloaddition processes. The component associated to the length of the C14−C15 bond, which is going from double to single bond, also has a small participation. Several bond angles and dihedral angles also participate in the TVs. These components are associated with the hybridization change that is developing in the C6, C14, and C15 centers to go from sp^2 to sp^3. Finally, the unappreciable participation of the components associated to the O7−Si8 bond length at **TS4** confirms the nonmigration of the trimethylsilyl group on the [5 + 2] cycloaddition process along the mode II.

The imaginary frequency values for these TSs are 455i, 492i, and 539i cm^{-1}, respectively. These imaginary frequencies are similar to those found for concerted [4 + 2] cycloaddition processes and are in agreement with the motion of heavy atoms involved in the cycloaddition process. For these cycloaddition processes there is a relationship between the relative energies and the imaginary frequency values; the most favorable TS has a lower imaginary frequency.

(iii) Bond Order and Charge Analysis. The extent of bond formation or bond breaking along a reaction pathway is provided by the concept of bond order (BO). This theoretical tool has been used to study the molecular mechanism of chemical reactions.[18] To follow the

(16) (a) Bachrach, S. M. *J. Org. Chem.* **1994**, *59*, 5027. (b) Houk, K. N.; Loncharich, R. J.; Blake, J. F.; Jorgensen, W. L. *J. Am. Chem. Soc.* **1989**, *111*, 9172.

(17) Since experimental activation parameters are not available for this [5 + 2] cycloaddition, the B3LYP/6-31G activation Gibbs energy can be compared with that found experimentally for the dimerization of cyclobutadiene at 127 °C ($\Delta G^{\ddagger}$ = 33.8 kcal/mol). (a) Benford, G. A.; Wassermann A. *J. Chem. Soc.* **1939**, 362. (b) Wassermann A. *Monatsh. Chem.* **1952**, *83*, 543.

(18) (a) Lendvay, G. *J. Mol. Struct. (THEOCHEM)* **1988**, *167*, 331. (b) Lendvay, G. *J. Phys. Chem.* **1989**, *93*, 4422. (c) Lendvay, G. *J. Phys. Chem.* **1994**, *98*, 6098.

Table 4. Imaginary Frequency (Frequency, cm^{-1}), Hessian Unique Negative Eigenvalue (Eigenvalue, au), Main Components of the Transition Vector (C, au), and Corresponding Geometric Parameters (G, Bonds in Å, Angles in Degrees) for the TSs Corresponding to the Intermolecular [5 + 2] Cycloaddition Processes of the γ-Pyrone 1

	TS2			**TS3**			**TS4**	
frequency	−454.6			−491.8			−539.2	
eigenvalue	−0.04322			−0.04928			−0.05820	
	C	**G**		**C**	**G**		**C**	**G**
C2−C14	0.624	2.276	C2−C14	0.704	2.092	C2−C14	0.623	2.180
C6−C15	0.669	2.224	C6−C15	0.565	2.357	C6−C15	0.651	1.933
C14−C15	−0.128	1.392	C14−C15	−0.133	1.393	C5−C6	−0.122	1.432
C5−C6−C15	−0.091	99.8	O1−C6−C15	−0.125	92.3	C14−C15	−0.158	1.421
O1−C6−C15	−0.137	92.9	C5−C6−C15	−0.081	94.1	O1−C6−C15	−0.124	97.1
C10−C6−C15	−0.085	106.3	C10−C6−C15	−0.060	108.6	C10−C6−C15	−0.104	106.4
C2−C15−C14−C13	0.120	−99.9	C2−C14−C15−H15	−0.222	112.8	C2−C15−C14−C13	0.125	−100.2
C2−C14−C13−H13	−0.118	104.5				C2−C14−C15−H15	0.158	−118.4
C2−C14−C15−H15	0.158	−108.5				C2−C14−C15−H15′	−0.134	103.6
C2−C14−C15−H15′	−0.146	98.9						

Table 5. Wiberg Bond Orders at 1, IN1, TS2, TS3, and TS4

	1	**IN1**	**TS2**	**TS3**	**TS4**
O1−C2	0.97	1.02	1.00	0.97	0.98
C2−C3	1.57	1.27	1.14	1.11	1.28
C3−C4	1.06	1.11	1.06	1.06	1.08
C4−C5	1.13	1.34	1.51	1.48	1.30
C5−C6	1.66	1.47	1.24	1.28	1.24
O1−C6	1.02	1.08	1.02	1.04	0.93
C3−O7	1.02	1.42	1.54	1.48	1.15
C4−O9	1.60	1.12	1.06	1.06	1.45
O7−Si8	0.51	0.06	0.05	0.04	0.46
Si8−O9	0.04	0.48	0.51	0.51	0.10
C2−C14	0.00	0.00	0.32	0.41	0.37
C6−C15	0.00	0.00	0.36	0.32	0.55
C14−C15	1.96	1.96	1.51	1.48	1.34

nature of the these processes, the Wiberg bond indices[19] have been computed by using the NBO analysis as implemented in Gaussian 98. The results are included in Table 5.

A comparison of the geometrical parameters and BOs at **1** and **IN1** indicates that the intermediate **IN1** has a molecular structure closer to the zwitterionic structures **II** to **IV** than the proposed oxidopyrylium ylide structure **I** (see Scheme 5). Thus, the C4−O9 BO value, 1.12, indicates a small π-character of the C4−O8 single bond, because of the delocalization the lone pair of the O9 oxygen atom on the carbocationic C4 center (structure **II**). Moreover, the C4−C5 and C5−C6 BO values, 1.34 and 1.47, respectively, indicate an allylic carbocation structure represented by the structures **III** and **IV**. Finally the low O1−C2 and O1−C6 BO values, in the range of 1.0−1.1, agree with a low participation of the structure **I**.

The BO analysis at the TSs corresponding to the [5 + 2] cycloadditions shows the synchronicity of the bond formation processes. For **TS2** the BO values for the C2−C14 and C6−C15 forming bonds are 0.32 and 0.36, respectively. These data indicate that this TS corresponds to a synchronous process, where the two σ-bonds are formed simultaneously. Moreover, the lower BO values found at this TS related with those for [4 + 2] cycloadditions indicates that this TS is earlier. For **TS3**, the BO values for the C2−C14 and C6−C15 forming bonds are 0.41 and 0.32, respectively. This TS is slightly less synchronous than **TS2** as a consequence of the constraints imposed by the tether. Finally, the most disadvantaged **TS4** presents a large asynchronicity for the bond formation process; the BO values of the C2−C14 and C6−C15 forming bonds are 0.37 and 0.55, respectively.

The natural population analysis for **TS2** and **TS3** allows us to understand the electronic nature of these cycloaddition processes. The atomic charges corresponding to the intramolecular process have been shared fragmenting the TSs along the C2−C11 single bonds. The values of the charge transfer from the alkene residue to the oxidopyrylium ylide system at **TS2** and **TS3** are 0.04 and 0.09 e, respectively, indicating a negligible charge transfer along these cycloadditions. These results are in agreeement with the FMO analysis for theses [5 + 2] cycloadditions, which indicates a more favorable $HOMO_{alkene}-LUMO_{oxidopyrylium\ ylide}$ interaction; and with the dipole moment values found for **1** (4.02 D), **TS1** (6.17 D), **IN1** (5.09 D), **TS2** (4.28 D), **TS3** (4.31 D), **2** (3.25 D), and **3** (3.22 D), which increases slightly in **TS1** and decreases on going to cycloadducts.

The bond order and natural population analysis suggest that these [5 + 2] cycloaddition processes take place via a pericyclic mechanism similar to that found for concerted [4 + 2] cycloadditions where the two σ-bonds are simultaneously formed.

Finally, solvent effects in these [5 + 2] cycloaddition processes have been estimated using a relatively simple self-consistent reaction field method[20] based on the polarizable continuum model of the Tomasi's group.[21] Single point calculations at the stationary points along the most favorable reactive channel give similar relative energies than those obtained in gas-phase calculations.[22] Inclusion of solvent effects increases 0.2 kcal/mol the relative energy of **TS2** because of a slightly larger stabilization of **1** compared to **TS2**.

Conclusions

In the present work we have carried out a theoretical study of the molecular mechanism for the intramolecular [5 + 2] cycloaddition of β-silyloxypyrones bearing tethered alkenes using ab initio methods. The PES for these cycloadditions has been explored, and four reactive pathways have been characterized by means of the

(19) Wiberg, K. B. *Tetrahedron* **1968**, *24*, 1083.

(20) (a) Tomasi, J.; Persico, M. *Chem. Rev.* **1994**, *94*, 2027. (b) Simkin, B. Y.; Sheikhet, I. *Quantum Chemical and Statistical Theory of Solutions-A Computational Approach*; Ellis Horwood: London, 1995.

(21) (a) Cances, M. T.; Mennunci, V.; Tomasi, J. *J. Chem. Phys.* **1997**, *107*, 3032. (b) Cossi, M.; Barone, V.; Cammi, R.; Tomasi, J. *Chem. Phys. Lett.* **1996**, *255*. (c) Barone, V.; Cossi, M.; Tomasi, J. *J. Comput. Chem.* **1998**, *19*, 404.

(22) As the solvent used in the experimental work is toluene, we have used its dielectric constant, $\epsilon = 2.38$.

Scheme 5

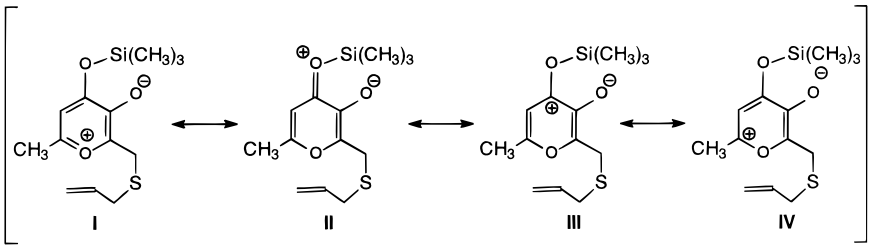

localization of the corresponding stationary points. Relative rates and stereoselectivity have been analyzed and discussed.

Analysis of the PES indicates that the reaction can take place along two reactive modes: in mode I, the initial migration of the neighboring silyl group to the carbonyl group of the γ-pyrone gives a weak oxidopyrylium ylide intermediate, which by a concerted intramolecular [5 + 2] cycloaddition affords the final cycloadduct. In mode II, the initial [5 + 2] cycloaddition on the γ-pyrone system followed by the concomitant migration of the silyl group affords the final cycloadduct. The barriers for the mode II are larger than those for the mode I, the cycloaddition for the γ-pyrone system being forbidden. These results suggest the necessity of the presence of the neighboring silyloxy to the carbonyl group in order for the cycloaddition to become feasible. Moreover, the large activation enthalpy associated with this cycloaddition demands an intramolecular process in order to minimize the unfavorable negative activation entropy. These intramolecular [5 + 2] cycloadditions are very stereoselective due to the constraints imposed by the tether.

Finally, a comparison of the energetic results obtained at different computational levels points out that the B3LYP/6-31G* results are similar to those obtained using the very expensive MP3/6-31G* calculations. Moreover, while the HF/6-31G* calculations give large barriers, those obtained using MP2/6-31G* are very low. This comparative study allows us to select the B3LYP/6-31G* computational level as the most appropriate for the study of this sort of cycloaddition reactions.

Acknowledgment. This work was supported by research funds provided by the Ministerio de Educación y Cultura of the Spanish Government by DGICYT (project PB98-1429). All calculations were performed on a Cray-Silicon Graphics Origin 2000 with 64 processors of the Servicio de Informática de la Universidad de Valencia. We are most indebted to this center for providing us with computer capabilities.

Supporting Information Available: Tables giving the total energies for the stationary points of the intramolecular [5 + 2] cycloaddition reaction of the γ-pyrone **1**, and the intermolecular [5 + 2] cycloaddition reaction of **IN4** + **5**. This material is available free of charge via the Internet at http://pubs.acs.org.

JO000061F